EUROPEAN ORGANIZATION FOR NUCLEAR RESEARCH

CERN-PPE/93-191
August 25, 1993

Results of a First Beam Test of Hadron Blind Trackers

M. Chen, D. Luckey, M. Smolin, K. Sumorok, X. Zhang
Laboratory for Nuclear Science, MIT, Cambridge, MA, USA

A. Bolozdynya, S. Belogurov, D. Churakov, A. Koutchenkov,
A. Kovalenko, V. Kuzichev, V. Lebedenko,
V. Sheinkman, G.Smirnov, G.Safronov, V. Vinogradov
ITEP, Moscow, Russia

Y. Giomataris, C. Joseph, M. Werlen
IPN, Lausanne University, Lausanne, Switzerland

G. Charpak
CERN, Geneva, Switzerland

B. Blumenfeld, A.K. Gougas, D. Steele
Johns Hopkins University, Baltimore, MD, USA

M. Akopyan
Institute for Nuclear Research, Moscow 117312, Russia

Abstract

We describe the experimental results of a new type of electron tracker, called Hadron Blind Detector or HBD. An HBD prototype was tested with gas mixtures of CF_4 with He or Ne and Parallel Plate Avalanche Chamber having a CsI photocathode of eight pads. Beam tests confirm the large Cherenkov light bandwidth over EUV region that can be obtained with such gas mixtures. It results in a large quality factor of about 500 cm^{-1} which allows HBD operation with much shorter radiator thickness than conventional Cherenkov counters. Full electron efficiency was obtained, while pions were rejected up to momenta of 9 GeV/c. HBD is unique to measure electron trajectories near the vertex, veto Dalitz pairs, and provide trigger on electrons among heavy hadron background. We discuss the use of such detectors for lepton identification and detection in high energy physics experiments and especially heavy ion colliders.

1 Introduction

In high intensity fixed target, beam dump, or colliding beam experiments using relativistic heavy ion or hadrons it is often required to detect e/γ precisely near the interaction regions in the presence of very large numbers of hadrons produced. For example, in the case of Au ion on Au ion collisions, the number of π's produced is about 10,000 particles/event and 2000 even at the central region with rapidity $|\eta| < 1$ at RHIC, and about five times larger at the Large Hadron Collider (LHC) energies. In a proton-proton collider, multiplicity is lower but pile-up of many events is expected, due to high luminosity, and coverage of the forward-backward rapidity region is required.

The main backgrounds for direct electrons are π^o Dalitz pairs, photon conversions and hadrons, while for direct photons they are mainly π^o/η decays. For muons, they are K decays before the hadron absorbers. A tracker which is sensitive only to electrons near the interaction regions can reconstruct the electron trajectories to obtain the secondary vertex.

The Hadron Blind Detector (HBD), originally proposed by G. Charpak and Y. Giomataris [1], uses Cherenkov light emitted by relativistic particles to identify electrons and to measure their trajectories. Its application to Heavy Ion Colliders to reject Dalitz pairs and its potential use in low temperature environment in combination with liquid Xenon or Krypton calorimeters to increase the pion rejection was introduced by [2].

HBD is useful for experiments emphasizing e/γ physics at heavy ion colliders, such as the PHENIX experiment at RHIC (see [3]) and L3H at LHC Heavy Ion Collider [4]. In the future proton-proton colliders electron identification provided by the calorimeter is limited by jets faking electrons. One can reject such events using low material and fast HBD trackers at an early trigger level [5].

HBD uses the same gas for both the radiator and the detection gap. Thus there is no longer a need for windows to separate the radiator region from the amplification/detector region. Such windows limit the transparency in the far UV for all Cherenkov counters. An active research was undertaken to find gas mixtures transparent in the extreme UV region (EUV) which can be used simultaneously as a detector gas filling having a high multiplication gain (10^5 - 10^6). Laboratory results have shown that CF_4 mixtures with noble gases may serve as ideal HBD gas [6]. Among the gas quenchers, CF_4 is one of the most transparent and the radiating Cherenkov light can be extended in the EUV region up to 12 eV.

The Cherenkov light emitted in the radiator is converted into photo-electrons by a thin CsI photocathode [7]. The photo-electrons produced are then amplified and collected by anode wires in a Parallel Plate Avalanche Chamber (PPAC), consisting of an anode wire plane and a plane of cathode pads. The spatial points of the electrons are obtained using the energy weighted average of signals from the anode wires and from the cathode pads. We describe herewith experimental results obtained with an

HBD prototype. We present extensive laboratory results, as well as tests in a particle beam.

2 Experimental set-up

The HBD prototype tested is shown in Fig. 1. It consists of the following components: a pressure tank, front flange with sapphire UV window at the center, a CsI photocathode, a PPAC and a back flange with gas, HV and signal ports. It permits operation at 10^{-10} < absolute pressure <5 atm and temperature down to -160 °C. The outgassing rate after baking at 50°C has been measured to be less than 10^{-7} m-bar/week.

HBD uses Cherenkov light generated in 40 cm of gas at room temperature. The Cherenkov light is converted into photo-electrons by a thin (0.5 μm) CsI photocathode (40x40 mm^2), divided into eight 4mm wide strips with separated read-out. The spatial positions of the electrons are obtained using the energy weighted average of signals from the cathode pads. The response of the cathode has been calibrated by a pulsed UV lamp system with 100 ns pulse width. The photo-electrons in turn are amplified and collected by anode wires in a PPAC. The cathode plane of the PPAC is the grounded CsI photocathode plate, the positive high voltage was applied on a anode wire mesh in a 4 mm gap.

Cathode strips of palladium-silver are deposited by sputtering technique on a 0.5 mm ceramic substrate. A thin 0.5 μm layer of CsI is then deposited by vacuum deposition of CsI powder. Since CsI is hydroscopic and water absorption can deteriorate its quantum efficiency, precautions were taken to minimize the exposure in atmospheric air. We estimate a 10 minutes total exposure of the coated photocathode in air. The photocathode was mounted inside the HBD volume immediately after the CsI deposition and HBD vessel was pumped down to the optimum vacuum before gas filling.

Gas purity of a few ppm is required to satisfy the demands for the radiator transparency in the EUV wavelength range. The gas purification system used (see Fig. 2) consists of an Oxisorb cartridge [1] and a primary-turbo pumping followed by an ion pump. Once a vacuum of about 10^{-5} Torr is obtained with the turbo system, a higher vacuum of 10^{-7} Torr is achieved with the ion pump. Although such high vacuum conditions are not required for the operation of the HBD, maximal precautions were taken to prevent any transparency losses in the radiator, since there was no on-line transparency monitor. Once a satisfactory vacuum level is reached the gas mixture is introduced passing through the filter. The gas filling is under control by a set of valves and allows operation at a broad range of pressures, from low pressure to overpressure.

[1] Oxisorb filters are made by Messer Griesheim GmbH, Dusseldorf, FRG

3 Search for HBD Gas Mixtures

The main goal of laboratory tests is to find gas mixtures which can achieve high and stable gain in a PPAC and which, as Cherenkov radiators, are highly transparent for < 220nm wavelengthes for which high quantum efficiency of CsI cathode has been measured. The prototype HBD has low outgassing and is vacuum tight, holding $< 10^{-7}$ Torr after one week. This is important since gas purity of a few ppm is required to achieve high transparency in the EUV wavelength range.

The detector response was measured using different gas mixtures at various partial pressures by applying a high voltage on the anode plane and measuring the cathode response when the cathode is illuminated by a pulsed or continuous UV lamp. The output signal resulting from the avalanche amplification process in the PPAC gap is fed to a charge preamplifier [8] in the case of pulsed operation mode. In the continuous mode the current was measured directly on a pAmp-meter.

Two types of UV lamps were used: a pulsed Xe + T_2 scintillating light source peaked at 172 nm and a continuous Hg lamp with quartz window. In the pulsed mode the observed current pulses are composed of a sharp peak due to electrons and a long tail due to the slow ion drift. The PPAC gain was measured at various electric field strengths by comparing the total collected charge to the one measured at lower voltages below the electron multiplication threshold. The collected charge reaches a plateau, at low electric fields and should be flat up to the threshold of the electron multiplication process; it reflects the fact that the total number of photoelectrons created in the CsI photocathode is fully collected on the anode. Above the multiplication threshold an exponential increase of the collected charge is measured as a function of the electric field. When CF_4 mixtures are used, however, a deep fall of the collected charge is observed just below the multiplication threshold. This drop is due to an electron capture phenomenon occurring when photoelectrons reach an energy of about 8 eV [9]. At 8 eV the electron absorption cross-section is of the order of 1 Mbarn which corresponds to an electron mean free path of the order of several mm (for a typical concentration of CF_4 of 10%). This absorption does not affect significantly the gain achieved. Since the chamber operates at high gain, charge multiplication occurs in a mean distance of 300 μm, which is much shorter than the electron mean free path.

Fig. 3 shows the gain obtained with various partial pressures of CF_4 at low pressure, as well as, gas mixtures of Neon and Helium with CF_4 at atmospheric pressure. A satisfactory gain of higher than 10^4 was obtained. Table 1 summarizes the maximum gain achieved with various gas mixtures at different partial pressures. Similarly, the multiplication factor is shown in Fig. 4 using a continuous light source. As indicated in Table 1 the best options are either pure CF_4 at various partial pressures or gas mixtures of a noble gas and CF_4. Using CH_4 instead of CF_4 one can achieve satisfactory gains, the transparency however, is much poorer. The gain limitation observed for some of the gas mixtures containing Ar or Kr as carrier gas is proba-

bly due to the photon feedback mechanism since these gases are scintillating in the bandwidth where CsI is sensitive (120 and 150 nm, respectively).

Since Neon and CF_4 are having high indices of refraction $(n-1) = 80 \times 10^{-6}$ and 400×10^{-6} respectively, the Cherenkov light production is higher compared to a helium gas mixture. We have performed the first beam tests with these two gas fillings: CF_4 or Ne+CF_4.

4 Beam Tests

A prototype of the detector was tested at a particle beam containing electrons/pions of 6-50 GeV/c. The first anode plane used wires of 50 μm diameter spaced every 800 μm and was found to produce non-uniform electric field. To improve the field homogeneity we have replaced the anode plane with a wire mesh plane composed of 50 μm wires interwoven every 500 μm.

The triggering system was composed of 3 plastic scintillators two placed in front of the apparatus and one behind it. The upstream counters had an active area of 3 x 3 cm^2, while the third one was 1.5 cm^2. A threshold Cherenkov counter was installed upstream of the whole setup to select pions or electrons. The gas filling was He at 3 atm ensuring a pion rejection up to 9 GeV/c. Two multiwire drift chambers placed one in front and one behind the HBD prototype were read out along with the HBD data providing us with a track information. Their space resolution is 150 μm. To increase the electron selection efficiency we have installed a BaF_2 crystal of 10 X_o downstream from the HBD. The electron trigger was provided by the coincidence signal of the 3 hodoscopes in conjunction with the threshold Cherenkov counter and the BaF_2 signals. To investigate the HBD pion rejection capabilities we have collected data using a pion trigger consisting of the coincidence of the 3 hodoscopes vetoed by the BaF_2 signal. The threshold Cherenkov was not used since its efficiency was approximately 10 %. Fig. 5 shows the schematic arrangement of the apparatus during the tests. We estimate that the pion contamination of the electron sample was approximately 2 %. The beam size spot was 15 mm diameter.

The HBD was filled with 250 mbar CF_4 partial pressure. The incident particle momentum was 6 GeV/c, below the pion Cherenkov threshold for both the HBD ($p_{thr} \approx 9$ GeV/c) and the threshold Cherenkov counter. At this gas pressure we expect that the Cherenkov angle θ is 15 mrad and the corresponding spot size at the photodetector plane is 12 mm diameter. Due to the Cherenkov angle of emission we expect that the signal coming from a particle above the Cherenkov threshold will be spread to several adjacent strips in the sensitive detector area. Fig. 6 shows the multiplicity of 4 mm wide strips for single particle events above the Cherenkov threshold.

The alignment was performed by varying the focusing magnets provided for the beam extraction. We had the possibility to independently change the horizontal and the vertical beam position. Fig. 7 shows the mean HBD response using both electron

and pion trigger. As one can see, the mean collected charge for pions remains flat for all values of horizontal and vertical beam displacement; while the corresponding electron curve exhibits a broad peak when the beam is aligned to the prototype. The higher absolute value of the mean collected charge is due to the Cherenkov light produced in the case of electrons, while the peak itself is due to the limited size of our photodetector (30 mm in diameter).

Using the track information from the two drift chambers we have rejected double tracks and plotted the HBD mean collected charge versus the horizontal (or vertical) track position. Again, the electron curve has a mean value that is 4-5 times higher than that of pions and is peaked at the HBD geometrical centre (Fig. 1). The charge distribution, for both electrons and pions, is shown in Fig. 8. Most of the pion collected charge is at the pedestal level confirming the insensitivity of the detector to minimum ionizing particles. The detector inefficiency at the pedestal is about 10 %. The number of detected photoelectrons is estimated to be > 4.

The number of photoelectrons N, produced in a photodetector is:

$$N = N_0 \cdot L \cdot \sin^2 \theta_C \tag{1}$$

where: L is the length of the radiator, θ_C is the Cherenkov emission angle and N_0 is a quality factor depending on the transparency of the radiator and the detector, and the photodetector quantum efficiency. In most Cherenkov counters a good quality factor is of the order of 100. We have observed a quality factor of 500. This is primary due to the fact that the wavelength range of sensitivity of our detector is not limited (as usually) by the window transparency cutoff, but extends up to the gas transparency cutoff which is 12 eV for CF_4 [10].

5 Future Improvement

As shown in Fig. 8 and Fig. 9, although a clear difference between pions and electrons has been observed, several factors should be improved to obtain much better e/π separation:

1. The high tail of the π spectrum is due to contamination of electrons and a better trigger is required,

2. The low tail of electrons is partly the result of non-uniformity in gain due to the woven mesh structure of the anode, which will be improved by using flat grid or very fine mesh,

3. Fluctuations due to the electron capture in CF_4 during the electron multiplication process [11]. This process requires more systematic investigation and it may be the cause of time fluctuations observed on the output HBD signal. One way to suppress such fluctuations is the use of a special filter, Nanochem

purifier, well known for being able to rid of electron negative components inside CF_4. Another way is the addition in the binary Ne+CF_4 gas mixture of a ternary gas. In a previous work it was demonstrated that the addition of a third component (CO_2 or H_2O) boosts the electron multiplication and has excellent thermolizing properties, resulting in a reduction of the fluctuations and suppression of the electron capture of the CF_4 [12]. In our case we need a far UV transparent third gas mixture. Candidates are Nitrogen and Hydrogen gases.

4. The expected number of photo-electrons produced by high energy electrons can be more than doubled by using 0.5 b of CF_4 + 0.5 b of Ne or 1 b of Ar + CH_4.

5. The use of fast amplifiers will enhance signals of the photo-electrons produced at the cathode relative to ions produced in the gap.

5.1 Conclusions and outlook

The results of the first particle beam test of a HBD prototype are encouraging: a large quality factor of 500 was obtained, far exceeding what have been achieved with conventional detectors. It confirms the first goal of the HBD concept: the absence of a window separating the Cherenkov radiator and the photon detector can improve the detected Cherenkov photon yield. To be sensitive to the EUV light, CF_4 based mixtures were used to increase the emitted photon bandwidth. Several mixtures, at low or atmospheric pressure, suitable for the HBD were tested. Admixture of Ne or He carrier gas with CF_4 are very promising. They combine high far UV transparency and stable and high gain for the PPAC detector. The electron capture effect during the avalanche development in CF_4 mixture is not a serious obstacle. It results in a small loss of about 10-30 % primary created photoelectrons, depending on the CF_4 concentration. Pure He or Ne gas mixtures exhibit a photoelectron back-diffusion process, which appears to decrease the quantum efficiency of CsI photocathodes by a factor of 2-3. This loss is recovered by the addition of a few % of the $CF_4(CH_4)$ quencher.

The second goal of the HBD concept was also demonstrated: the quite low efficiency of the PPAC on the primary ions created in the gas by minimum ionizing particles. Depending on the gas admixture used and the gain of the PPAC, this inefficiency was of the order of 10-30%. Full efficiency was measured for high energy incident electrons. The pion rejection capability of the device was limited by a broad pulse height distribution, larger than the expected statistical fluctuations, observed in the electron sample. This effect, as well as the time instabilities of the output signal observed for some CF_4 gas mixtures, is under study. It could be due to two effects: electric field inhomogeinities near the anode mesh or/and fluctuations during the avalanche process due the CF_4 electron capture effect. Further experimental investigations are needed to improve the photodetector, the electronic chain and the

gas mixture. The quantum efficiency of CsI cathodes could be improved by using better polished surfaces, as used in previous investigations [13]. Better electric uniformity can be reached by using very fine meshes. We expect the optimization of such different components should allow to obtain a fully efficient HBD in the next years.

5.2 Acknowledgements

We are grateful to S. Aronson, S.Nagamiya, Y. Akiba, R. Hayano, T. Hemmick, and Nu Xu for their encouragement and support as well as many useful discussions. We are indebted to our colleagues from the L3-SMD collaboration, in particular R.Leiste, T. Coan and B.Zhou, for providing us with the data acquisition system during the SPS tests. This work is partially supported by DOE Grant # DE-FG02-93ER40790 and by the PHENIX Collaboration.

References

[1] Y. Giomataris and G.Charpak, Nucl. Instr. and Meth. A310(1991)589

[2] M. Chen et al., Proceedings of International Conference on Liquid Radiation Detector, Waseda University, April 1992, also PHENIX Workshop, BNL, Aug. 24, 1992.

[3] PHENIX Conceptual Design Report, January 29, 1993.

[4] M. Chen, L3H A Muon-Electron-Photon Detector for LHC Heavy Ion Physics, CERN/LHCC/93-15.

[5] Y. Giomataris and G.Charpak, Proc. of the International Lepton Photon Symposium and Europhysics Conference, Geneva July 1991, 2(1991)251.

[6] Y. Giomataris et al., Nucl. Instr. and Meth. A323(1992)431

[7] J. Seguinot et al., Nucl. Instr. and Meth. A297(1990) 133

[8] J.Fischer et al., Nucl. Instr. and Meth. A238(1985)249

[9] S.R. Hunter and L.G. Christophorou. J.Chem. Phys. 80(12)1984; L. G. Christophorou et al., J. Appl. Phys.71 (1992) 15: J. Va'vra, Nucl. Instr. and Meth. A323(1992)34

[10] W.R.Harshbarger et al., J.Electron Spectrosc., 1(1972/73)319.

[11] S.F.Biagi, Nucl. Instr. and Meth. A310(1991)133.

[12] P.G. Daskos, J.G.Carter and L.G. Christoforou, J.Appl. Phys. 71(1)1992

[13] G. Charpak et al. CERN/PPE/92-220, submitted to Nucl. Instr. and Meth.

Table 1: Maximum stable gain and HV reached for various HBD gases and gaps between anode and cathode

gas mixture	pressure, bar	gap, mm	max gain	voltage, kV
CF_4	0.35	3	10^5	5.15
	0.25	4	10^5	4.7
	0.15	4	5×10^7	3.1
	0.05	4	1.5×10^8	1.45
CH_4	0.5	4	10	5.5
He+4%CF_4	1.0	4	10^4	3.05
Ar+4%CF_4	1.0	4	1	4.8
Ar+1%CF_4	1.0	4	1	3.5
Ar+0.5%CF_4	2.0	4	1	4.0
	1.0	4	2	3.35
Ar+1%CH_4	1.0	4	1	3.8
	0.5	4	1	2.5
Ar+1%CF_4+1%CH_4	1.0	4	3	3.9
Ne+4%CF_4+21%He	1.0	4	10	4.7
Kr+10%CF_4	0.2	4	5×10^3	2.0
Kr+20%CF_4	0.22	4	10^3	2.3

List of Figures

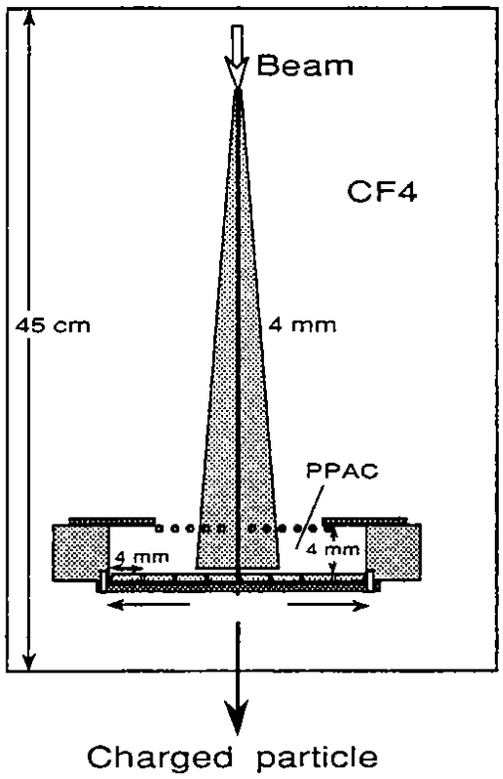

Figure 1: Schematic of a single cell of a hadron blind tracker. A charged particle (e^-) produces Cherenkov light in a gas radiator, producing photoelectrons on the photocathode, which are extracted, amplified and collected on the anode grid and readout using both the anode wires and the cathode pads to obtain the electron spatial positions.

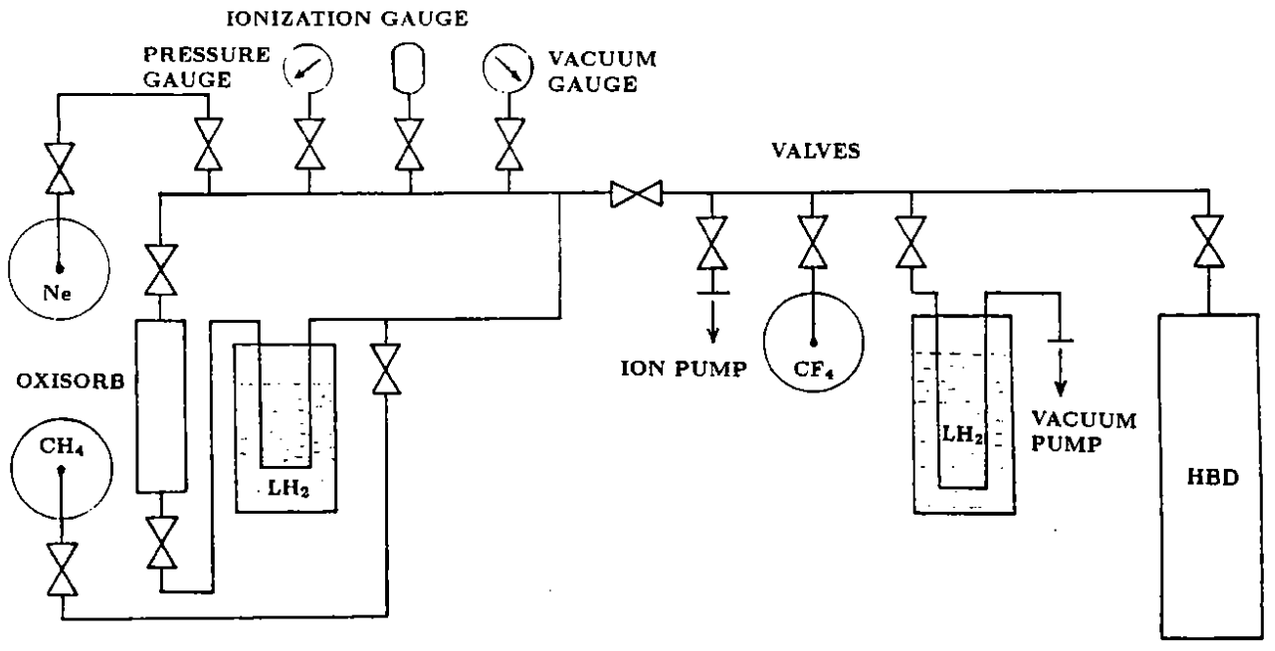

Figure 2: The gas purification system. Using high vacuum, gas impurities are removed; then the chamber is filled with low (or atmospheric) pressure gas under the control of the gas filling system (V).

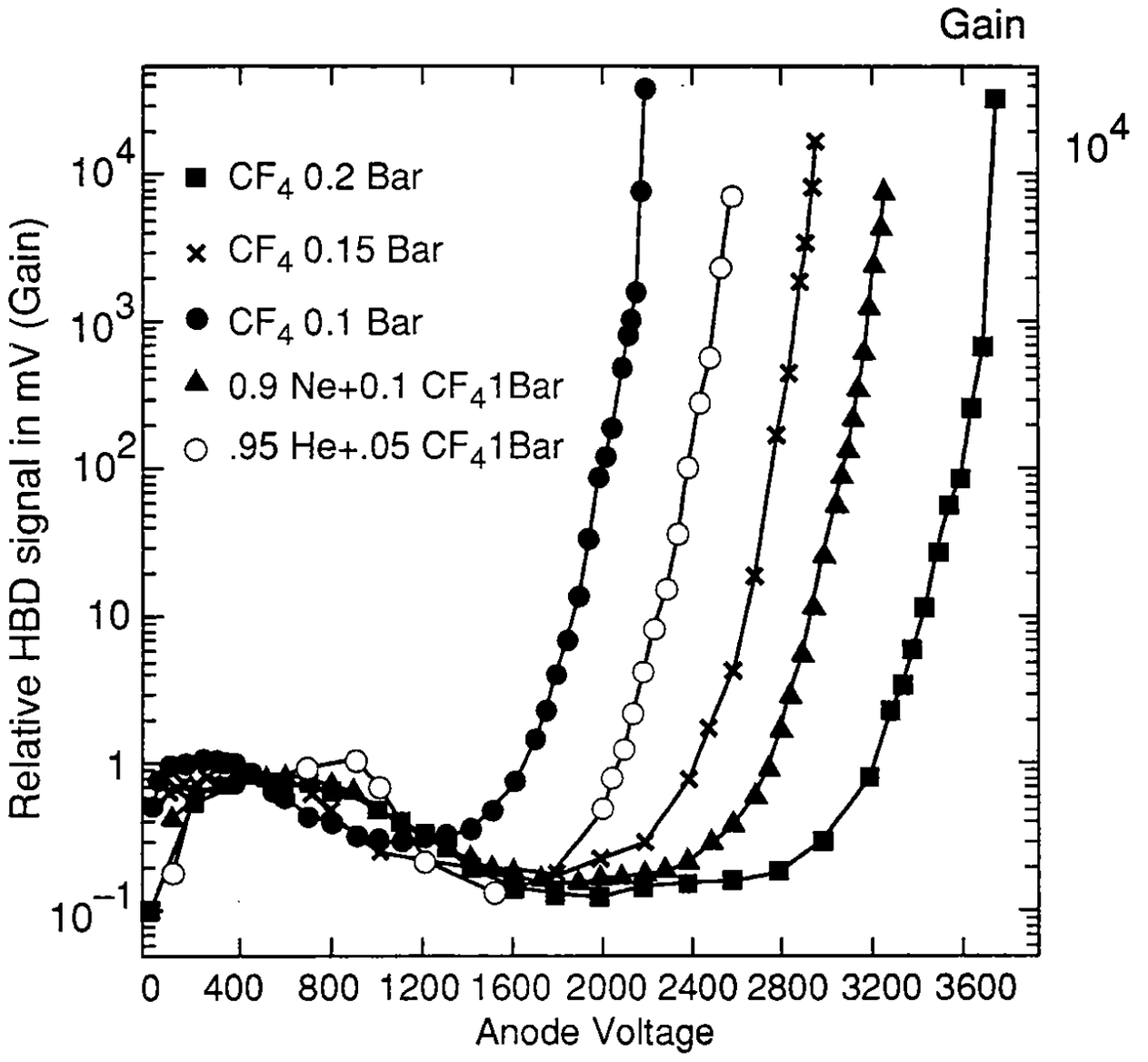

Figure 3: The measured AC current gain versus high voltage across a 4 mm gap for various gas mixtures in an HBD.

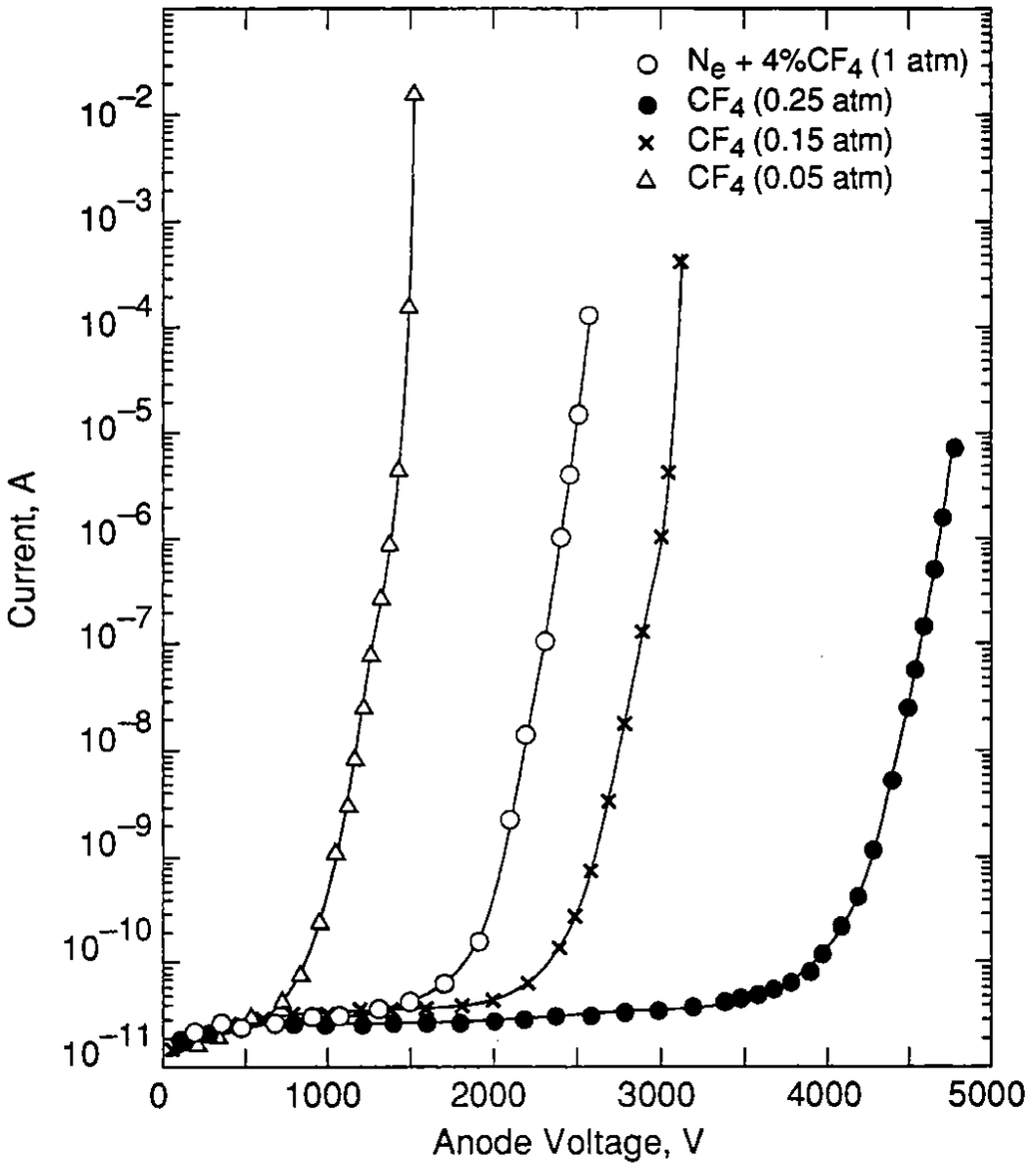

Figure 4: The measured DC current gain versus high voltage across a 4 mm gap for various gas mixtures in an HBD.

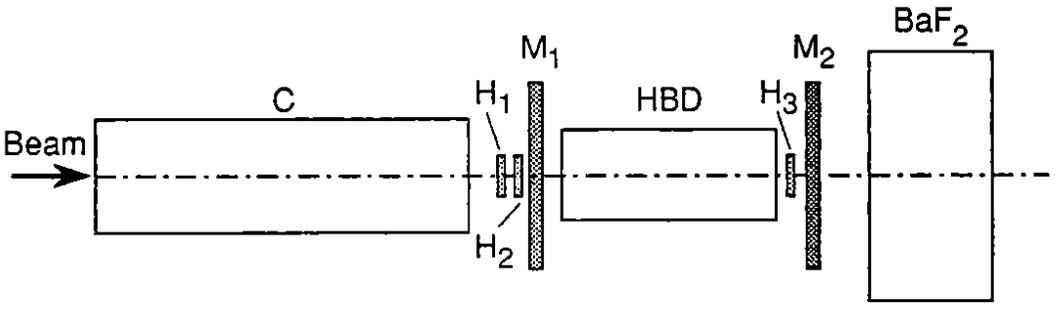

Figure 5: The schematic drawing of the PS beam setup. The HBD prototype is placed behind a threshold Cherenkov counter (C), two plastic scintillator hodoscopes (H_1, H_2) and a MWPC (M_1). Downstream from the HBD is the H_3 counter, a MWPC (M_2) and a 20 cm long BaF_2 crystal

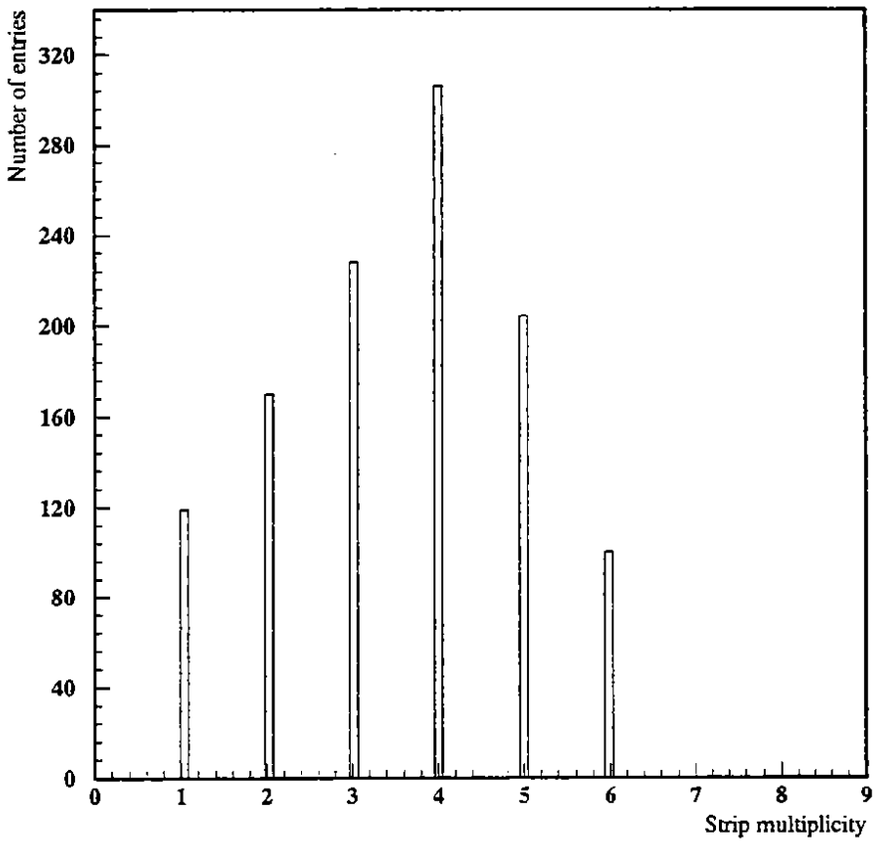

Figure 6: Distribution of the number of 4 mm wide cathode pads fired by the Cherenkov light of 6 GeV electrons.

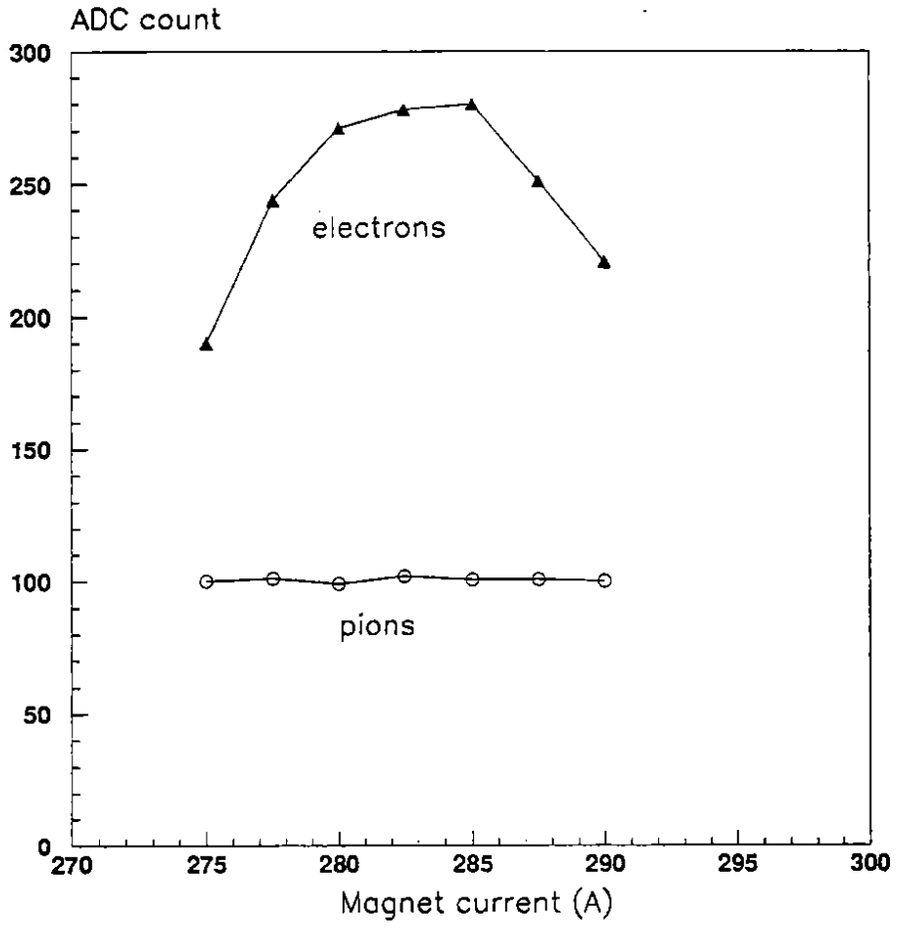

Figure 7: Mean collected charge vs. the vertical beam position for electrons and pions. Pedestal, about 70 ADC counts, has not been subtracted.

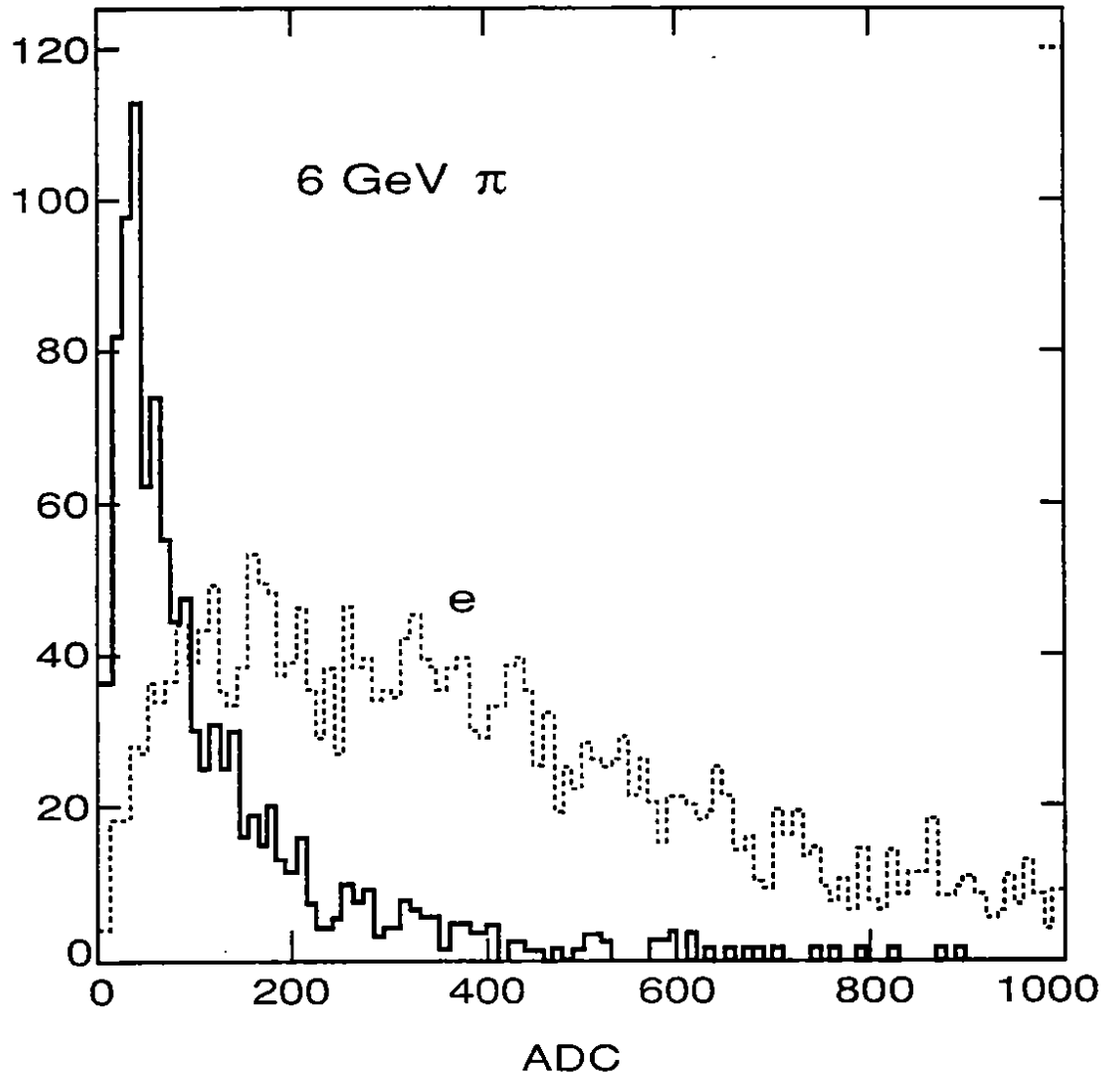

Figure 8: The measured ADC distributions for 6 GeV electrons and π's, from the test HBD, filled with 0.2 b of CF_4.

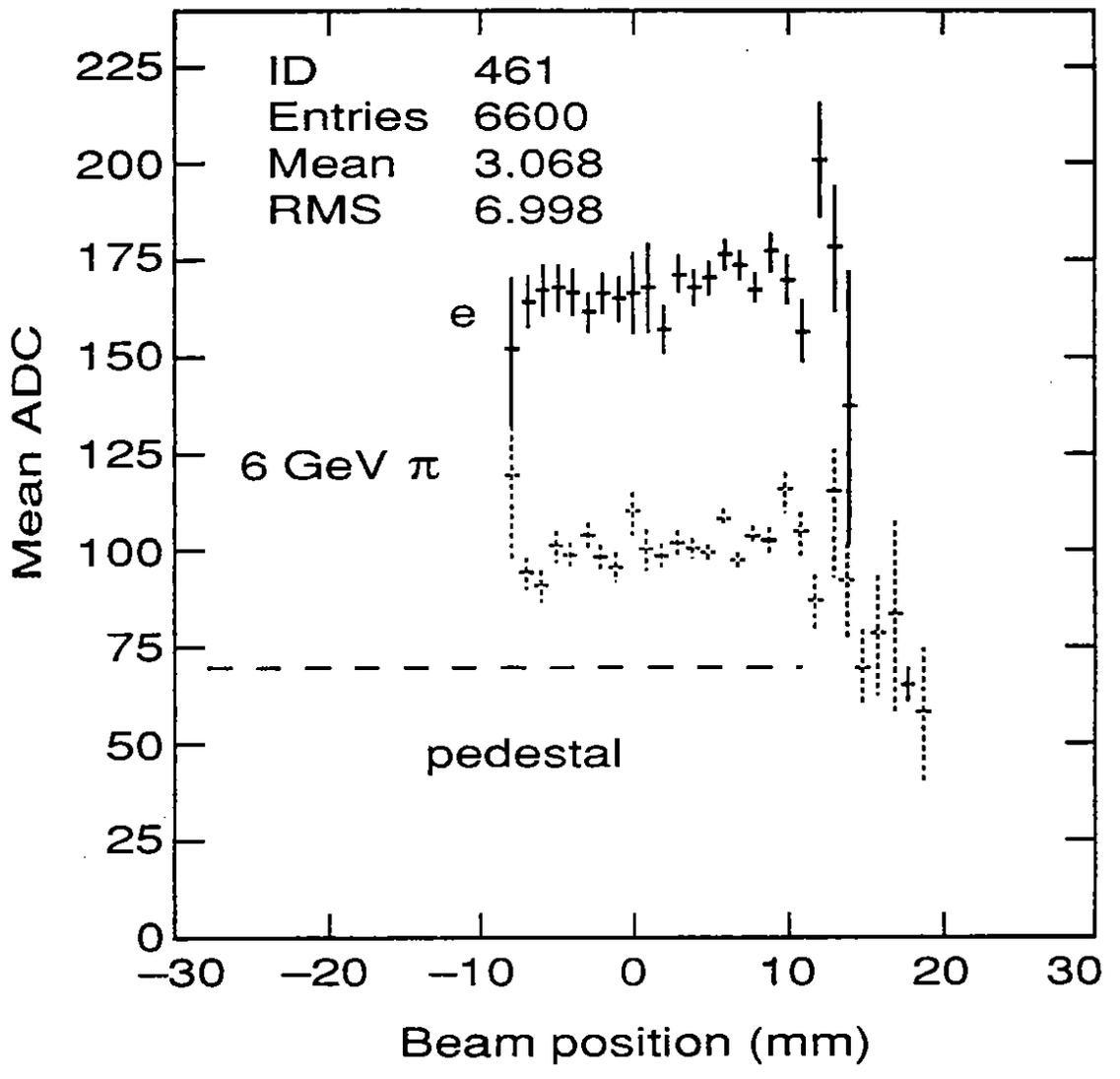

Figure 9: The measured mean ADC values for 6 GeV electrons and π's, versus the transverse beam position across the test HBD, filled with 0.2 b of CF_4.